

Chye Yann (Orcid ID: 0000-0001-9470-4241)  
Kaag Anne Marije (Orcid ID: 0000-0001-5696-5758)  
London Edythe (Orcid ID: 0000-0003-3577-7808)  
Verdejo-Garcia Antonio (Orcid ID: 0000-0001-8874-9339)

## **Subcortical surface morphometry in substance dependence: An ENIGMA addiction working group study**

Yann Chye<sup>1</sup>, Scott Mackey<sup>2</sup>, Boris A Gutman<sup>3</sup>, Christopher R K Ching<sup>4</sup>, Albert Batalla<sup>5,6</sup>, Sara Blaine<sup>7</sup>, Samantha Brooks<sup>8</sup>, Elisabeth Caparelli<sup>9</sup>, Janna Cousijn<sup>10</sup>, Alain Dagher<sup>11</sup>, John J Foxe<sup>12</sup>, Anna E Goudriaan<sup>13,14</sup>, Robert Hester<sup>15</sup>, Kent Hutchison<sup>16</sup>, Neda Jahanshad<sup>4</sup>, Anne M Kaag<sup>10</sup>, Ozlem Korucuoglu<sup>17</sup>, Chiang-Shan R Li<sup>7</sup>, Edythe D London<sup>18</sup>, Valentina Lorenzetti<sup>1,19</sup>, Maartje Luijten<sup>20</sup>, Rocio Martin-Santos<sup>6</sup>, Shashwath Meda<sup>21</sup>, Reza Momenan<sup>22</sup>, Angelica Morales<sup>18</sup>, Catherine Orr<sup>3</sup>, Martin P Paulus<sup>23,24</sup>, Godfrey Pearlson<sup>7</sup>, Liesbeth Reneman<sup>25</sup>, Lianne Schmaal<sup>26</sup>, Rajita Sinha<sup>7</sup>, Nadia Solowij<sup>27,28</sup>, Dan J Stein<sup>8</sup>, Elliot A Stein<sup>9</sup>, Deborah Tang<sup>11</sup>, Anne Uhlmann<sup>8</sup>, Ruth van Holst<sup>26</sup>, Dick J Veltman<sup>29</sup>, Antonio Verdejo-Garcia<sup>1</sup>, Reinout W Wiers<sup>9</sup>, Murat Yücel<sup>1</sup>, Paul M Thompson<sup>4</sup>, Patricia Conrod<sup>30</sup>, Hugh Garavan<sup>2</sup>

1. Brain and Mental Health Research Hub / Addiction and Mental Health Program, Monash Institute of Cognitive and Clinical Neurosciences, School of Psychological Sciences, Monash University, Australia
2. Departments of Psychiatry and Psychology, University of Vermont, USA
3. Biomedical Engineering, Illinois Institute of Technology, Chicago, IL, USA
4. Imaging Genetics Center, Mark & Mary Stevens Institute for Neuroimaging & Informatics, Department of Neurology, Keck School of Medicine, University of Southern California, Marina del Rey, CA, USA
5. Department of Psychiatry, Brain Center Rudolf Magnus, University Medical Centre Utrecht, The Netherlands
6. Department of Psychiatry and Psychology, Hospital Clinic, IDIBAPS, CIBERSAM, Institute of Neuroscience, University of Barcelona, Spain
7. Departments of Psychiatry and Neuroscience, Yale University School of Medicine, CT, USA

This is the author manuscript accepted for publication and has undergone full peer review but has not been through the copyediting, typesetting, pagination and proofreading process, which may lead to differences between this version and the Version of Record. Please cite this article as doi: [10.1111/adb.12830](https://doi.org/10.1111/adb.12830)

8. SA MRC Unit on Risk & Resilience in Mental Disorders, Dept of Psychiatry and Neuroscience Institute, University of Cape Town, South Africa
9. Neuroimaging Research Branch, Intramural Research Program, National Institute of Drug Abuse, USA
10. Department of Developmental Psychology, University of Amsterdam, The Netherlands
11. Brain Imaging Center, Montreal Neurological Institute, McGill University, Canada
12. Department of Neuroscience & The Ernest J. Del Monte Institute for Neuroscience, University of Rochester School of Medicine and Dentistry, NY, USA
13. Amsterdam UMC, Department of Psychiatry, Amsterdam Institute for Addiction Research, University of Amsterdam, The Netherlands
14. Arkin Mental Health Care, Amsterdam, The Netherlands
15. Melbourne School of Psychological Sciences, University of Melbourne, Australia
16. Department of Psychology and Neuroscience, University of Colorado Boulder, CO, USA
17. Department of Psychiatry, Washington University School of Medicine, MO, USA
18. Jane and Terry Semel Institute of Neuroscience and Human Behavior, David Geffen School of Medicine, University of California at Los Angeles, CA, USA
19. School of Psychology, Faculty of Health Sciences, Australian Catholic University, Australia
20. Behavioural Science Institute, Radboud University, the Netherlands
21. Hartford Hospital/IOL, Olin Neuropsychiatry Research Center, Hartford, CT, USA
22. Clinical NeuroImaging Research Core, Division of Intramural Clinical and Biological Research, National Institute of Alcohol Abuse and Alcoholism, USA
23. VA San Diego Healthcare System and Department of Psychiatry, University of California San Diego, CA, USA
24. Laureate Institute for Brain Research, OK, USA
25. Department of Radiology and Nuclear Medicine, Amsterdam UMC, location AMC, the Netherlands
26. Department of Psychiatry, University of Amsterdam, the Netherlands
27. School of Psychology and Illawarra Health and Medical Research Institute, University of Wollongong, Australia

28. The Australian Centre for Cannabinoid Clinical and Research Excellence (ACRE),  
Australia
29. Department of Psychiatry, VU University Medical Center, the Netherlands
30. Department of Psychiatry, Université de Montreal, CHU Ste Justine Hospital, Canada

**Corresponding author:** Professor Hugh Garavan, Department of Psychiatry, University of  
Vermont, Burlington, VT, 05405, USA

Tel: 802-656-9618, Email: hugh.garavan@uvm.edu

**Running title:** subcortical shape in addiction

**Word count**

Abstract: 250 words

Article body: 4645 words

Number of figures: 5

Number of tables: 2

Supplementary information: 1

**ABSTRACT**

While imaging studies have demonstrated volumetric differences in subcortical structures associated with dependence on various abused substances, findings to date have not been wholly consistent. Moreover, most studies have not compared brain morphology across those dependent on different substances of abuse to identify substance-specific and substance-general dependence effects. By pooling large multi-national datasets from 33 imaging sites, this study examined subcortical surface morphology in 1,628 non-dependent controls and 2,277 individuals with dependence on alcohol, nicotine, cocaine, methamphetamine, and/or cannabis. Subcortical structures were defined by FreeSurfer segmentation and converted to a mesh surface to extract two vertex-level metrics – the radial distance (RD) of the structure surface from a medial curve and the log of the Jacobian determinant (JD) – that respectively describe local thickness and surface area dilation/contraction. Mega-analyses were performed on measures of RD and JD to test for the main effect of substance dependence, controlling for age, sex, intracranial volume, and imaging site. Widespread differences between dependent users and non-dependent controls were found across subcortical structures, driven primarily by users dependent on alcohol. Alcohol dependence was associated with localized lower RD and JD across most structures, with strongest effects in the hippocampus, thalamus, putamen, and amygdala. Meanwhile, nicotine use was associated with greater RD and JD relative to non-smokers in multiple regions, with strongest effects in the bilateral hippocampus and right nucleus accumbens. By demonstrating subcortical morphological differences unique to alcohol and nicotine use, rather than dependence across all substances, results suggest substance-specific relationships with subcortical brain structures.

**Keywords:** addiction; structural MRI; substance dependence

**Abbreviations:** AlcD = alcohol dependence; NicD = nicotine dependence; CocD = cocaine dependence; MetD = methamphetamine dependence; CbD = cannabis dependence; RD = radial distance; JD = log of the Jacobian determinant; ICV = intracranial volume

## INTRODUCTION

Substance dependence is characterized by compulsive substance-seeking, and a loss of control over intake, despite negative social, interpersonal, and occupational consequences <sup>1</sup>. Substance use disorder can be related to any of a number of licit and illicit substances, including alcohol, cannabis, opioids, stimulants, and tobacco <sup>1</sup>. While not all substance users will experience problems related to use, a significant number will become dependent, although the proportion differs between substances. Within the US alone, over 1.5 million substance users are admitted to treatment facilities every year for problems related to substance use <sup>2</sup>, reflecting a huge personal cost, and a severe toll on social and economic development. Substance dependence accounts for over 37.6 million disability-adjusted life years (DALYs; i.e., number of years lost due to disability and premature mortality) globally <sup>3</sup>. Disability (mental health, social and emotional functioning) also increases with dependence severity among users <sup>4</sup>. Identifying biomarkers associated with dependence across different substances (i.e. alcohol, tobacco, cannabis, opioids, stimulants) may greatly help our understanding of dependence and its consequences, and improve the identification of individuals most vulnerable to dependence-related harm.

Neuroimaging research over the years has attempted to elucidate brain-based biomarkers (i.e. structure, function, and neurochemistry) that may indicate aberrant processes in dependence on various substances <sup>5</sup>. Separately, these studies have demonstrated volumetric differences in common subcortical structures, including the hippocampus, amygdala, striatum, and thalamus, in opioid, stimulant, alcohol, tobacco, and cannabis use disorders <sup>6-10</sup>. Such findings are consistent with the proposed role of these striatal and limbic structures in supporting processes (e.g., planning and decision making, reward, and memory) crucially involved in the etiology of substance use and dependence <sup>11,12</sup>. However, studies have yet to compare subcortical structure across multiple substances using the same methods, making it difficult to infer substance-specific versus substance-general neural alterations characterizing dependence. Furthermore, gross volumetric measures commonly employed by structural imaging studies may be unable to capture more localized subcortical differences (i.e. focal differences on the vertices or triangular mesh that make up the subcortical surface, as

opposed to a single volumetric value across the entire structure) that can either be generalizable across substances of abuse or specific to particular substances. This is relevant as structures such as the hippocampus, amygdala, and striatum may be functionally segregated across their subregions and/or topology, given differences in gene expression, receptor distributions (e.g. GABA<sub>A</sub>, dopamine, and cannabinoid receptors, and innervation along the structure <sup>13-19</sup>. Different regions of these subcortical structures may therefore be differentially associated with substance use and dependence. For example, the basolateral and central amygdala are differentially recruited over the course of cocaine-seeking in rats <sup>20</sup>. The former is suggested to be relevant for the development of substance-seeking 'habit', while the latter is thought to be responsible for its long-term maintenance, reflecting unique but complementary roles in the etiology of substance use <sup>20</sup>. The dorsal and ventral regions of the hippocampus are also differentially implicated in context-induced and cue-induced reinstatement of substance use, due to their greater involvement in cognitive and affective functions respectively <sup>16,21,22</sup>. Different substances of abuse are further thought to have differing cellular and molecular pathways to dependence, raising the potential of substance-specific dependence effect <sup>23</sup>. These observations motivated us to consider more fine-grained shape differences in subcortical morphology when delineating individual substance dependence-related effects on the brain.

This study was conducted by the Addiction working group of the Enhancing NeuroImaging Genetics through Meta-Analysis (ENIGMA) Consortium, which leverages already collected neuroimaging datasets to overcome limitations of sample size and statistical power in identifying biomarkers of substance dependence <sup>24,25</sup>. Our previous study examining FreeSurfer-segmented subcortical volumes across a combined sample of 23 research sites identified substance-specific effects of alcohol dependence in the amygdala, hippocampus, nucleus accumbens, and putamen <sup>26</sup>. A nonlinear support vector machine was further able to classify alcohol dependence and nicotine dependence above chance levels (despite there being no significant nicotine dependence effects on individual subcortical volumes), suggesting that there may be nonlinear or multivariate patterns of effects across multiple brain areas not captured by standard univariate analysis of regional volumes. Building on this

result, this study sought to characterize substance-general and substance-specific shape variation across the subcortical surfaces, which might better identify fine-grained regional effects not captured by a single volumetric measure (i.e. as was the limitation of our previous paper, Mackey *et al.*, 2018). This study contained pooled neuroimaging data from 33 research sites, adopting a surface-based approach used to quantify subcortical shape variability (i) between all dependent users and non-dependent controls, (ii) across dependence groups (alcohol, nicotine, cocaine, methamphetamine, or cannabis) and non-dependent controls, and (iii) across nicotine use status. This will provide insight into whether dependence on different substances of abuse may be associated with unique and localised effects on the brain, specifically on subcortical structures. In turn, such brain effects may have the potential to serve as useful biomarkers for risk factors or evidence of recovery from substance dependence.

## **MATERIALS AND METHODS**

Case and control data were contributed from 33 scanning sites from the ENIGMA addiction working group <sup>25</sup>; <http://enigmaaddiction.com>). This included a total of 1,535 non-dependent controls, and 2,270 individuals with a primary substance dependence diagnosis (according to DSM-IV criteria) on one of five substances: alcohol (AlcD), nicotine (NicD), cocaine (CocD), methamphetamine (MetD), and cannabis (CbD), although ~8% of dependent users met criteria for dependence on more than one substance. Cases were excluded if criteria were met for any lifetime history of central nervous system disease, or a current axis I diagnosis apart from substance dependence, apart from mood and anxiety disorders. Non-dependent controls may have used these substances (i.e. mainly alcohol and nicotine), but did not meet diagnostic criteria or were not assessed for substance dependence. Individual site information and diagnostic instrument is provided in Supplementary Table 1. All subjects provided written informed consent, and all procedures were in accordance with the Declaration of Helsinki.

### ***MRI Data Processing***

Site-specific scanner and acquisition details for T1-weighted MR images are available in Supplementary Table 1. All scans were prepared (either centrally at the University of Vermont or at the respective individual sites) using the FreeSurfer image analysis environment (<http://surfer.nmr.mgh.harvard.edu/>) version 5.3.0, to segment 14 subcortical regions (i.e., bilateral accumbens, amygdala, caudate, hippocampus, pallidum, putamen, and thalamus) from surrounding brain tissue. All FreeSurfer output underwent quality control at each site, according to an established protocol (<http://enigma.ini.usc.edu/protocols/imaging-protocols/>), which included outlier detection and visual inspection of all data. A second level of quality control was also performed on a random selection of participants from each site, centrally at the University of Vermont.

Morphometric analysis on the FreeSurfer-segmented subcortical regions was performed at the University of Vermont. This entailed converting subcortical boundaries to a mesh surface using the Medial Daemons method<sup>27,28</sup>; <http://enigma.ini.usc.edu/ongoing/enigma-shape-analysis/>). This step includes registration of the FreeSurfer-segmented subcortical structures to a master template based on brain images from 200 young adults created by the University of Southern California's Imaging Genetics Center team. By matching their shape curvatures and medial features to a master template, mesh representations of the subcortical boundaries were generated. All resulting mesh reconstructions were visually inspected by Y.C. for quality control. Reconstructions that had significant artifacts (e.g. spikes, holes) or were grossly inaccurate upon visual inspection (2.19% of generated structures) were excluded. Finally, two vertex-level metrics were derived from the mesh surface, to quantify subcortical shape. This included (i) the radial distance (RD), which is the distance between each surface vertex and a skeleton core created along the long axis of the structure; and (ii) the natural logarithm of the Jacobian determinant (JD), which represents the surface dilation ratio necessary to map corresponding vertices on the subject-specific surface to the surface of the master template. The logarithm is used to obtain a distribution that is closer to Gaussian. RD and JD capture surface measures akin to 'thickness (from a central skeleton)' and 'area' respectively.<sup>29</sup>, and are only weakly correlated (i.e., correlation coefficient from our sample,  $r = .0228$ ,  $CI = [.0226, .0230]$ ). They thus complement each other in providing information

on localized grey matter changes across subcortical structures. The number of vertices per structure was consistent across subjects, as defined by the master template (accumbens = 930; amygdala = 1368; caudate = 2502; hippocampus = 2502; putamen = 2502; thalamus = 2502; pallidum = 1254). See **Fig. 1** for an overview of the vertex-wise shape metrics employed.

### *Statistical Analysis*

Three sets of tests examined substance-general and substance-specific correlates of dependence, using an optimized split-half strategy, described in the later paragraph. The first set (model I: substance-general model) assessed the main effect of dependence on any substance (i.e., dependent users vs. non-dependent control). In these analyses, individuals reporting dependence on one or more substance were included.

The second set (model II: substance-specific model) assessed the main effect of individual substances of dependence (i.e. AlcD, NicD, CocD, MetD, CbD, versus non-dependent controls as a fixed factor with 6 levels). In the second set of analyses, individuals who were dependent on more than one substance were excluded, to clarify the association between dependence on individual substances and subcortical morphology. However, non-dependent occasional substance use (e.g. recreational alcohol use in either group) was not excluded. Effect of AlcD was further validated in a post-hoc analysis with a subsample of 171 AlcD participants versus non-dependent controls, to ensure that any observed AlcD effects were not due to their comparatively larger sample (n=830) relative to other substance-user groups in this study (n=171-565). The subsample of 171 AlcD participants were created by systematically selecting one in five AlcD participants, ordered by site, sex, and age, to ensure that these covariates were matched across selected and non-selected samples.

The third set of analyses (model III: nicotine-disambiguation model) investigated nicotine use effects. The large number of non-dependent controls and individuals diagnosed with dependence who use nicotine may have affected the search for nicotine-related results in the second model. This is particularly important as individual studies that recruited users on AlcD, CocD, MetD, and CbD may not necessarily screen for nicotine use or dependence.

Consequently, the third set of analyses compared three groups: individuals with NicD, non-dependent controls who use nicotine, and non-dependent controls who do not use nicotine.

Similar to the method in our previous paper<sup>26</sup>, data for the three models were analysed using an optimized split-half strategy whereby the data were first split into two halves matched for site, age, sex, and intracranial volume. Subsequently, the series of linear models were tested on each separate half, on the RD and JD measures of each subcortical structure, controlling for participants' age, sex, intracranial volume (ICV, to account for premorbid head size), and imaging site. All outputs were corrected using a regional searchlight false discovery rate (FDR) method<sup>30</sup> at  $q = .05$ , conservatively treating the 14 subcortical structures (i.e., bilateral accumbens, amygdala, caudate, hippocampus, pallidum, putamen, and thalamus) and two metrics (RD and JD) in each model as a single family of tests. Lastly, the corresponding outputs across the split halves were overlaid to identify common regions of significance (i.e., vertices that were significant across both splits, henceforth referred to as 'overlap').

## RESULTS

Demographic information for the full sample is presented in **Table 1**. In general, dependent samples included more males, were older, and exhibited greater ICV than non-dependent controls. Association between sex, age, and ICV are also presented graphically in Supplementary Figures 1 and 2. To control for these factors, sex, age, and ICV were included as covariates in the linear models. The effects of sex, age, and ICV on RD and JD are also presented graphically in Supplementary Figure 3.

### *Model I: Substance-general Model*

Dependent users were compared to non-dependent controls. On average, dependent users exhibited lower RD and JD values relative to non-dependent controls in the hippocampus and amygdala, diffuse areas of the thalamus, and the right nucleus accumbens (**Fig. 2**).

### *Model II: Substance-specific Model*

For this model, individuals with dependence on multiple substances (~8%) were excluded, resulting in a reduced sample size of 1,535 non-dependent controls and 2,085 dependent users. No significant differences emerged from comparisons of NicD vs. non-dependent controls, CocD vs. non-dependent controls, MetD vs. non-dependent controls, or CbD vs. non-dependent controls. However, AlcD demonstrated significantly smaller RD and JD values, particularly across bilateral hippocampus and putamen, and the right amygdala and thalamus (**Fig. 3**). These regions of significance roughly correspond to regions identified in Model I. Post-hoc analysis on a smaller subsample of 171 AlcD participants (i.e. the sample size of the smallest substance dependence group in our study) similarly showed significantly smaller RD and JD values relative to non-dependent controls, suggesting that the observed alcohol-specific effect was not due to the comparatively larger AlcD sample relative to other substance-user groups in our study (n=171-565).

### ***Model III: Nicotine-disambiguation Model***

Finally, model III was run to clarify the potential effect of NicD, by minimizing the potential confounding influence of cigarette smoking in non-dependent controls. Control participants recruited from all sites were separated into 918 non-smoking controls, 189 smoking controls, after excluding participants without information on smoking status. These groups, and the group of 565 NicD participants that were originally recruited by sites that tested for smoking effects, were compared. NicD participants demonstrated significantly higher RD and JD values relative to non-smoking controls, indicating greater volume and surface area across bilateral regions of the hippocampus, thalamus, putamen, and the right nucleus accumbens (**Fig. 4**).

Similarly smoking controls (who were not assessed for nicotine dependence by the recruiting sites) demonstrated inflated structures relative to non-smoking controls, across the hippocampus, thalamus, diffuse regions of the putamen, and the right nucleus accumbens (**Fig. 5**). There was no significant difference between NicD and smoking controls.

Common regions of significance across both splits (i.e., overlap) are reported in Table 2 as the percentage of significant vertices relative to the total number of vertices across each structure.

## DISCUSSION

Our previous volumetric mega-analysis of individuals dependent on one of five substances (alcohol, nicotine, cocaine, methamphetamine, and cannabis) found lower amygdala, hippocampus, nucleus accumbens, and putamen volume in alcohol dependent relative to non-dependent controls, but no subcortical associations specific to dependence on any of the other substances<sup>26</sup>. The current follow-up investigation adopts a more sensitive measure that allows the quantification of localized differences at the vertex-level to closely examine subcortical surface changes that may not have been detectable in our previous study. In a larger combined sample of 3,805 individuals, we demonstrated lower RD and JD values consistent with lower thickness and surface area in subcortical structures associated with substance dependence, mainly along the hippocampus, amygdala, thalamus, and accumbens, across substances of abuse. Such differences were driven by alcohol dependence and no subcortical differences were observed for cocaine, methamphetamine, or cannabis users in relation to non-dependent controls, in agreement with our previous paper<sup>26</sup>. Further examination of nicotine dependence relative to non-smoking controls, and smoking controls relative to non-smoking controls, surprisingly demonstrated an inverse association of higher RD and JD values consistent with greater thickness and greater surface area across the hippocampus, thalamus, and right accumbens in both nicotine dependence and smoking controls relative to non-smoking controls.

The striking alcohol-specific effect on subcortical structures (in particular, the striatal and limbic structures) is consistent with our previous ENIGMA study on gray matter volume in substance dependence, which demonstrated lower volume in widespread cortical and subcortical regions specific to alcohol dependence<sup>26</sup>. The absence of a subcortical association with cocaine, methamphetamine, and cannabis is interesting given the literature

implicating striatal and limbic structures in the development of dependence towards these substances<sup>7,31</sup>. To ensure that the observed alcohol-specific effect was not due to the comparatively larger alcohol dependence sample (n=830) relative to other substances (n=171-565) in our study, we re-ran the substance-specific model with a subsample of 171 alcohol dependence users. Results remained consistent and significant, suggesting that alcohol dependence effect was robust, even across a much smaller sample. The individual effects of other illicit substances on brain morphology may be subtler than previously assumed<sup>6,7,10</sup>. Alternatively, various moderating influences such as quantity of substance use and timed developmental exposure may be relevant in considering brain morphology as alcohol use typically starts earlier than the other illicit drugs (e.g. 50% of those who ever used alcohol starts at age 14-21, compared to age 16-28 for cannabis and cocaine<sup>32</sup>). Unfortunately, comparison of use level across different substances was not possible in the present samples, as similar substance use histories were not obtained on all subjects at the participating sites. An important goal for future studies will be to examine the impact of age of onset and lifetime quantity of use on morphological measures in alcohol dependence.

While nicotine dependence effects were not observed in Model II when segregating users into their substance of choice, differences were observed in Model III when comparing nicotine-dependent users to non-smoking controls. The lack of effect of the former model may be due to the confounding influence of smoking status within the non-dependent control sample. Control samples collected by sites that seek to examine the effect of other illicit substances (e.g. cannabis, cocaine, methamphetamine) often do not account for smoking status in their samples or deliberately seek to match groups on cigarette use levels. By segregating non-smoking and smoking controls, Model III sought to tease apart the influence of occasional cigarette smoking relative to dependence. Finding greater RD and JD in nicotine-dependent users relative to non-smoking controls in the hippocampus, putamen, and thalamus, was in agreement with studies linking greater putamen volume with cigarette smoking<sup>33,34</sup>, but in contrast to previous evidence of smaller thalamus and hippocampus in chronic cigarette smokers relative to non-smokers<sup>35-37</sup>. Some studies have also reported no thalamic or hippocampal volume difference in smokers relative to non-smokers<sup>34,38</sup>, reflecting the

inconsistency of current evidence on nicotine dependence. By pooling a combined sample of 1,672 subjects, adopting a more sensitive measure of vertex-level morphology, and requiring split-half replication, this study provides evidence for a reinterpretation of cigarette smoking-related effects on brain morphology. The smoking-related effect was not only observed between nicotine dependence and non-smoking controls, but also between smoking controls (who were not diagnosed with a nicotine dependence) and non-smoking controls, suggesting structural differences associated with use rather than dependence. The proposed exposure-related effect (as opposed to dependence-related effect) of cigarette smoking is supported by a study demonstrating a dose-dependent relationship between nicotine use and enlarged putamen volume<sup>33</sup>. Nicotinic receptors, that are particularly densely located along regions where effects were observed (i.e. hippocampus, thalamus, basal ganglia)<sup>39</sup>, and are paradoxically upregulated in response to chronic nicotine exposure<sup>40,41</sup>, may underlie the observed morphological differences.

It is interesting to note that similar cigarette-smoking related effects (i.e. greater RD and JD in the hippocampus, thalamus, and putamen) are not apparent in other substance-dependent users in our sample, given the high comorbidity between cigarette smoking and other substance use, particularly cannabis<sup>42,43</sup>. Subcortical morphometry may be subject to an interactive effect between nicotine and other substance use. For example, the typically observed subcortical differences in users dependent on methamphetamine, cocaine, or cannabis<sup>6,7,10</sup> may have been counteracted by an opposing cigarette-smoking effect. Unfortunately, the low number of methamphetamine-, cocaine-, or cannabis-dependent subjects who are also non-smokers, and the lack of well-characterized smoking level information within these substance-dependent users prevents an interrogation of the interactive effect between cigarette smoking and other substance use/dependence in brain structural effects.

A key structure emerging from this comprehensive examination of substance-related subcortical morphology is the hippocampus, being notably implicated (up to >40% of the structure's surface) across the examined models. The hippocampus is a crucial structure for

learning and memory - its function is central to substance-related memory processes including reinforcement learning and reinstatement of substance use <sup>44</sup>. The observed hippocampal effect was mostly confined to the hippocampal head and inferior body of the left hippocampus, roughly coinciding with the *cornu ammonis* (CA1) and subicular regions <sup>45</sup>. The CA1 is thought to be important for input integration, and contains a high density of *N*-methyl-D-aspartate (NMDA) receptors that are modulated by substance use, in particular alcohol <sup>46,47</sup>. Alcohol-associated NMDA effects are further thought to contribute to alcohol tolerance and dependence <sup>47</sup>. The subiculum receives input from the CA1, and along with the CA1, provides the main hippocampal outflow to a range of cortical and subcortical sites <sup>45</sup>. Both the CA1 and subiculum are particularly affected in neurodegenerative disorders such as Alzheimer's disease <sup>48</sup>, reflecting regional vulnerability to age-related atrophy, that may further be amplified by chronic alcohol abuse <sup>49</sup>. Further, the anterior thalamic sub-region was also found in this study to be preferentially affected relative to other sub-regions of the thalamus. The anterior thalamus is primarily connected to the hippocampus and frontal cortex, with reduced thalamo-frontal projections and anterior thalamic volume being particularly associated with increased age and cognitive (attention and memory) decline <sup>50,51</sup>. The selective vulnerability of the anterior thalamus may further extend to alcohol dependence, as demonstrated by this study.

While effects observed in the amygdala were relatively small and diffuse, across both the lateral and basal regions <sup>52</sup>, they were observed mostly in the right amygdala. This laterality effect is in line with previous studies demonstrating a stronger association between the right (vs. left) amygdala with substance dependence <sup>53</sup>, and risk for developing alcohol dependence <sup>54</sup>. Findings from the latter study also suggest that an amygdala effect may precede dependence. The basolateral amygdala, implicated in our study, is also argued to be important for reward learning, motivation, and decision making, and therefore relevant in the early stages and acquisition of substance dependence (whereas the central amygdala is thought to be more involved in stress, negative reinforcement and maintenance of dependence) <sup>20,55,56</sup>. However, it should be noted that the cross-sectional nature of this study prevents us from confirming a causal role of subcortical differences across the trajectory of

substance dependence. Large scale, longitudinal studies that track the trajectory of brain development and substance use, such as the ABCD study (<https://abcdstudy.org/>) will be beneficial in clarifying the direction of association between substance use, dependence, and brain morphology.

The current findings should be interpreted in the light of several limitations. First, the datasets from multiple sites were collected under differing protocols and scanner sequences. The diagnostic instruments adopted by the imaging sites for segregating dependence from controls also differ. While these instruments are all validated and reliable, the inter-site differences may limit the specificity of study findings. This study attempted to mitigate the site issues in scanning and diagnosis by having a single rater visually inspect all subcortical reconstructions and by incorporating site factors in all the statistical models. Conversely, a benefit of making inference from multi-site data means that findings might have greater generalizability to the wider population, due to the collation of larger samples<sup>57</sup>. A second concern of adopting a multi-site approach is in the interpretability of findings, particularly in relation to the spectrum of dependence severity, lifetime use quantity, or other clinical variables of interest such as those that index quality of life and wellbeing. The latter is particularly relevant for their potential confounding influence on observed brain differences. For example depressive symptoms and mood disorders, which are highly comorbid in substance dependence<sup>58</sup>, have also been associated with alterations of subcortical volumes (e.g., reduction in hippocampal volumes)<sup>59</sup>. However, as not all sites in the current study collected information on depressive symptoms, or adopted common instruments in measuring them, their confounding influence on the current study findings cannot be ruled out. Moving forward, a standardized approach to recruiting and testing future samples (i.e., wherein all future substance dependence studies should collect information on duration, frequency, and quantity of substance use, and mood and anxiety symptoms, at the minimum) will be beneficial to allow for standardization and comparisons across datasets. This approach may in turn facilitate collaboration and crosstalk across studies, in clarifying substance-general and substance-specific brain correlates.

To conclude, our comprehensive examination of subcortical morphology in the largest dependent user sample to date revealed significant alcohol and nicotine-specific effects on subcortical structures, in particular the hippocampus, thalamus, and putamen. By contrast, the effect of illicit substance dependence on brain volume was found to be minimal. Such findings might warrant a revised understanding of the structural correlates of addiction. It is possible that the brain-based effects of illicit substances may not be evident with morphological measurements, but may instead be confined to functional or connectivity-related differences.

## Acknowledgements

We thank the ENIGMA Addiction Working Group for contributing the data necessary for this work, and the ENIGMA Shape Analysis Team for developing the shape pipeline used in this work. We also thank the Queensland Twin Imaging (QTIM) Study (Drs. Margie Wright, Greig de Zubicaray, and Katie McMahon) for contributing the master template from which the shape pipeline was developed.

## Funding

This work was supported in part by National Institutes of Health (NIH) grant U54 EB020403 from the Big Data to Knowledge (BD2K) program. Dr. Y Chye was supported by the Monash Bridging Postdoctoral Fellowship. Data collection: Dr. CRK Ching was supported by grants NIA T32AG058507, NIH/NIMH 5T32MH073526, and NIH grant U54EB020403. Dr. J Cousijn and Dr. AE Goudriaan received funding for the Cannabis Prospective Study from Netherlands Organization for Health Research and Development (ZonMW) grant 31180002 from Netherlands Organization for Scientific Research (NWO). Dr. A Dagher received support from the Canadian Institutes for Health Research. Dr. H Garavan and Dr. JJ Foxe received funding from the National Institute on Drug Abuse (NIDA) grant R01-DA014100. Dr. AE Goudriaan and Dr. RJ van Holst received funding from ZonMW grant 91676084 from NWO. Dr. O Korucuoglu received support for the neuro-ADAPT study from the VICI grant 453.08.001 from the NWO, awarded to Dr RW Wiers. Dr CR Li received funding from NIDA grants R01AA021449, R01DA023248, and K25DA040032. Dr. ED London received support from NIH grants DA15179, DA022539, and DA024853, F30 DA021961 (KB), and MOI-RR-00865 (UCLA GCRC); endowments from the Katherine K. and Thomas P. Pike Chair in Addiction Studies and Marjorie M. Greene Trust, Philip Morris USA UCLA contract 20063287, and institutional training grants T32 DA 024635 (support of Angelica Morales) and T32 MH17140 (support of Golnaz Tabibnia). Dr. M Luitjen and Dr. DJ Veltman received support from the VIDI grant 016.08.322 from NWO, awarded to Ingmar HA Franken. Dr. R. Momenan received support from the National Institutes of Alcohol Abuse and Alcoholism (NIAAA)/NIH intramural research funding ZIA AA000123-02 to the Clinical NeuroImaging Research Core. Dr. A Morales received support from NIDA grant T32 DA024635. Dr MP Paulus received funding from National Institute of Mental Health (NIMH) grant R01 DA018307. Dr. G. Pearlson received funding from the NIDA grant R01 DA020709, and the NIAAA grants AA016599 and AA19036. Dr. R. Martin-Santos received support from Plan Nacional sobre Drogas. Ministerio de Sanidad y Política Social grant PNSD:2011/050 and SGR:2014/1114. Dr. L. Reneman received funding from the Netherlands Organisation for health Research and development 40-00812-98-11002. Dr. L Schmaal and Dr. DJ Veltman received funding from ZonMW grant 31160003 from NWO. Dr. R Sinha received funding from NIDA (PL31-1DA024859-01), NIH National Center for

Research Resources (UL1-RR24925-01), and NIAAA grant (R01-AA013892). Dr. Z Sjoerds and Dr. DJ Veltman received funding from ZonMW grant 31160004 from NWO. Dr. N Solowij received support from the Clive and Vera Ramaciotti Foundation for Biomedical Research, the National Health and Medical Research Council Project grant 459111 and Australian Research Council Future Fellowship FT110100752. Dr. D Stein received support from the South African Medical Research Council. Dr. EA Stein received support from the Intramural Research Program of the National Institute on Drug Abuse (NIH). Dr. M Yücel received support from the National Health and Medical Research Council Fellowship 1117188 and the David Winston Turner Endowment Fund.

### **Competing Interests**

The authors report no competing interest. Dr. CRK Ching and Dr. PM Thompson receives partial research support from Biogen, Inc. (Boston), for research unrelated to the topic of this manuscript. Dr. M Yücel has received funding from Monash University, and Australian Government funding bodies such as the National Health and Medical Research Council (NHMRC), the Australian Research Council (ARC), and the Department of Industry, Innovation and Science. He has also received philanthropic donations from the David Winston Turner Endowment Fund, as well as payment from law firms in relation to court and/or expert witness reports.

### **Data Accessibility**

The summary data on which the analyses were performed are available from the corresponding author upon reasonable request.

### **Authors contribution**

PMT, PC, HG, and SM designed the study. BG and CRKC designed the study's method. AB, SB, SB, EC, JC, AD, JJF, AEG, RH, KH, NJ, AMK, OK, CSRL, EDL, VL, ML, RMS, SM, RM, AM, CO, MPP, GP, LR, LS, RS, NS, DJS, EAS, DT, AU, RVH, DJV, AVG, RWW, and MY collected the data. YC analysed the data with supervision from SM and HG. YC wrote the first draft with close input from SM and HG. All other authors provided intellectual feedback on the final draft.

**REFERENCES**

1. American Psychiatric Association. *Diagnostic and Statistical Manual of Mental Disorders, Fifth Edition (DSM-5)*. Arlington, VA: American Psychiatric Publishing; 2013.
2. Substance Abuse and Mental Health Services Administration C for BHS and Q. *Treatment Episode Data Set (TEDS): 2005-2015. State Admissions to Substance Abuse Treatment Services*. BHSIS Seri. Rockville, MD: Substance Abuse and Mental Health Services Administration; 2017.
3. Whiteford HA, Degenhardt L, Rehm J, et al. Global burden of disease attributable to mental and substance use disorders □: findings from the G  
*Lancet*. 2013;1575-1586. doi:10.1016/S0140-6736(13)61611-6
4. Grant BF, Saha TD, Ruan WJ, et al. Epidemiology of DSM-5 drug use disorder - Results from the national epidemiologic survey on alcohol and related conditions-III. *JAMA psychiatry*. 2016;73(1):39-47. doi:10.1001/jamapsychiatry.2015.2132
5. Garrison KA, Potenza MN. Neuroimaging and biomarkers in addiction treatment. *Curr Psychiatry Rep*. 2014;16(12):513. doi:10.1007/s11920-014-0513-5
6. Meyerhoff DJ. Structural neuroimaging in polysubstance users. *Curr Opin Behav Sci*. 2017;13:13-18. doi:10.1016/j.cobeha.2016.07.006
7. Hall MG, Alhassoon OM, Stern MJ, et al. Gray matter abnormalities in cocaine versus methamphetamine-dependent patients: a neuroimaging meta-analysis. *Am J Drug Alcohol Abuse*. 2015;41(4):290-299. doi:10.3109/00952990.2015.1044607
8. Durazzo TC, Meyerhoff DJ, Nixon SJ. Chronic Cigarette Smoking: Implications for Neurocognition and Brain Neurobiology. *Int J Environ Res Public Health*. 2010;7:3760-3791. doi:10.3390/ijerph7103760
9. Yang X, Tian F, Zhang H, et al. Cortical and subcortical gray matter shrinkage in alcohol-use disorders: a voxel-based meta-analysis. *Neurosci Biobehav Rev*. 2016;66(37):92-103. doi:10.1016/j.neubiorev.2016.03.034
10. Lorenzetti V, Chye Y, Silva P, Solowij N, Roberts CA. Does regular cannabis use affect neuroanatomy? An updated systematic review and meta-analysis of structural neuroimaging studies. *Eur Arch Psychiatry Clin Neurosci*. 2019. doi:10.1007/s00406-019-00979-1
11. Redish AD, Jensen S, Johnson A. A unified framework for addiction: vulnerabilities in the decision process. *Behav Brain Sci*. 2008;31(4):415-437; discussion 437-487. doi:10.1017/S0140525X08004986

12. Koob GF. Neurobiological substrates for the dark side of compulsivity in addiction. *Neuropharmacology*. 2009;56:18-31. doi:10.1016/j.neuropharm.2008.07.043
13. Small SA, Schobel SA, Buxton RB, Witter MP, Barnes CA. A pathophysiological framework of hippocampal dysfunction in ageing and disease. *Nat Rev Neurosci*. 2011;12(10):585-601. doi:10.1038/nrn3085
14. Balderston NL, Schultz DH, Hopkins L, Helmstetter FJ. Functionally distinct amygdala subregions identified using DTI and high-resolution fMRI. *Soc Cogn Affect Neurosci*. 2015;10(12):1615-1622. doi:10.1093/scan/nsv055
15. Haber SN. Corticostriatal circuitry. *Dialogues Clin Neurosci*. 2016;18(1):7-21. doi:10.1002/bit.260190307
16. Fanselow MS, Dong HW. Are the Dorsal and Ventral Hippocampus Functionally Distinct Structures? *Neuron*. 2010;65(1):7-19. doi:10.1016/j.neuron.2009.11.031
17. Fritschy J-M, Mohler H. GABAA-receptor heterogeneity in the adult rat brain: Differential regional and cellular distribution of seven major subunits. *J Comp Neurol*. 1995;359:154-194.
18. Herkenham M, Lynn AB, Little MD, et al. Cannabinoid receptor localization in brain. *Proc Natl Acad Sci U S A*. 1990;87(5):1932-1936. doi:10.1073/pnas.87.5.1932
19. Camps M, Cortes R, Gueye B, Probst A, Palacios JM. Dopamine receptors in human brain: Autoradiographic distribution of D2 sites. *Neuroscience*. 1989;28(2):275-290.
20. Murray J, Belin-Rauscent A, Simon M, et al. Basolateral and central amygdala differentially recruit and maintain dorsolateral striatum-dependent cocaine-seeking habits. *Nat Commun*. 2015;6:10088. doi:10.1038/ncomms10088
21. Degoulet M, Rouillon C, Rostain JC, David HN, Abiraini JH. Modulation by the dorsal, but not the ventral, hippocampus of the expression of behavioural sensitization to amphetamine. *Int J Neuropsychopharmacol*. 2008;11(4):497-508.
22. Rogers JL, See RE. Selective inactivation of the ventral hippocampus attenuates cue-induced and cocaine-primed reinstatement of drug-seeking in rats. *Neurobiol Learn Mem*. 2007;87(4):688-692.
23. Gupta S, Kulhara P. Cellular and molecular mechanisms of drug dependence: An overview and update. *Indian J Psychiatry*. 2007;49(2):85-90.
24. Thompson PM, Stein JL, Medland SE, et al. The ENIGMA Consortium: large-scale collaborative analyses of neuroimaging and genetic data. *Brain Imaging Behav*. 2014;8(2):153-182. doi:10.1007/s11682-013-9269-5

25. Mackey S, Kan K, Chararani B, et al. Genetic imaging consortium for addiction medicine: From neuroimaging to genes. *Prog Brain Res.* 2016;224:203-223.  
doi:10.1016/bs.pbr.2015.07.026
26. Mackey S, Allgaier N, Chararani B, et al. Mega-analysis of gray matter volume in substance dependence: General and substance-specific regional effects. *Am J Psychiatry.* October 2018.  
doi:10.1176/appi.ajp.2018.17040415
27. Gutman BA, Wang Y, Rajagopalan P, Toga AW, Thompson PM. Shape matching with medial curves and 1-D group-wise registration. In: *9th IEEE International Symposium on Biomedical Imaging (ISBI).* ; 2012:716-719.
28. Gutman BA, Madsen SK, Toga AW, Thompson PM. A family of fast spherical registration algorithms for cortical shapes. In: Shen L, Liu T, Yap P-T, Huang H, Shen D, Westin C-F, eds. *Multimodal Brain Imaging Analysis.* Springer International Publishing; 2013:246-257.  
doi:10.1007/978-3-319-02126-3\_24
29. Wang Y, Song Y, Rajagopalan P, et al. Surface-based TBM boosts power to detect disease effects on the brain: An N=804 ADNI study. *Neuroimage.* 2011;56(4):1993-2010.  
doi:10.1016/j.neuroimage.2011.03.040
30. Langers DRM, Jansen JFA, Backes WH. Enhanced signal detection in neuroimaging by means of regional control of the global false discovery rate. *Neuroimage.* 2007;38:43-56.  
doi:10.1016/j.neuroimage.2007.07.031
31. van de Giessen E, Weinstein JJ, Cassidy CM, et al. Deficits in striatal dopamine release in cannabis dependence. *Mol Psychiatry.* 2017;22(1):68-75. doi:10.1038/mp.2016.21
32. Degenhardt L, Chiu WT, Sampson N, et al. Toward a global view of alcohol, tobacco, cannabis, and cocaine use: findings from the WHO World Mental Health Surveys. *PLoS Med.* 2008;5:e141. doi:07-PLME-RA-0801 [pii] 10.1371/journal.pmed.0050141
33. Das D, Cherbuin N, Anstey KJ, Sachdev PS, Easteal S. Lifetime cigarette smoking is associated with striatal volume measures. *Addict Biol.* 2012;17(4):817-825.  
doi:10.1111/j.1369-1600.2010.00301.x
34. Yu R, Zhao L, Lu L. Regional grey and white matter changes in heavy male smokers. *PLoS One.* 2011;6(11). doi:10.1371/journal.pone.0027440
35. Durazzo TC, Meyerhoff DJ, Nixon SJ. Interactive effects of chronic cigarette smoking and age on hippocampal volumes. *Drug Alcohol Depend.* 2013;133(2):704-711.  
doi:10.1016/j.drugalcdep.2013.08.020

36. Gallinat J, Meisenzahl E, Jacobsen LK, et al. Smoking and structural brain deficits: a volumetric MR investigation. *Eur J Neurosci*. 2006;24(6):1744-1750. doi:10.1111/j.1460-9568.2006.05050.x
37. Sutherland MT, Riedel MC, Flannery JS, et al. Chronic cigarette smoking is linked with structural alterations in brain regions showing acute nicotinic drug-induced functional modulations. *Behav Brain Funct*. 2016;12(1):1-15. doi:10.1186/s12993-016-0100-5
38. Brody AL, Mandelkern MA, Jarvik ME, et al. Differences between smokers and nonsmokers in regional gray matter volumes and densities. *Biol Psychiatry*. 2004;55(1):77-84. doi:10.1016/S0006-3223(03)00610-3
39. Rubboli F, Court JA, Sala C, et al. Distribution of nicotinic receptors in the human hippocampus and thalamus. *Eur J Neurosci*. 1994;6:1596-1604. doi:10.1111/j.1460-9568.1994.tb00550.x
40. Nashmi R, Xiao C, Deshpande P, et al. Chronic nicotine cell specifically upregulates functional  $\alpha 4^*$  nicotinic receptors: Basis for both Tolerance in midbrain and enhanced long-term potentiation in perforant path. *J Neurosci*. 2007;27(31):8202-8218. doi:10.1523/jneurosci.2199-07.2007
41. Govind AP, Vezina P, Green WN. Nicotine-induced upregulation of nicotinic receptors: Underlying mechanisms and relevance to nicotine addiction. *Biochem Pharmacol*. 2009;78(7):756-765. doi:10.1124/dmd.107.016501.CYP3A4-Mediated
42. Degenhardt L, Lynskey MT, Hall WD. Alcohol, cannabis and tobacco use and the mental health of Australians: A comparative analysis of their associations with other drug use, affective and anxiety disorders, and psychosis. *Addiction*. 2001;96:1603-1614. doi:10.1080/09652140120080732
43. Subramaniam P, McGlade EC, Yurgelun-Todd DA. Comorbid cannabis and tobacco use in adolescents and adults. *Curr Addict Reports*. 2016;3(2):182-188. doi:10.1007/s11065-015-9294-9.Functional
44. Robbins TW, Ersche KD, Everitt BJ. Drug addiction and the memory systems of the brain. *Ann N Y Acad Sci*. 2008;1141:1-21. doi:10.1196/annals.1441.020
45. Van Leemput K, Bakkour A, Benner T, et al. Automated segmentation of hippocampal subfields from ultra-high resolution in vivo MRI. *Hippocampus*. 2009;19(6):549-557. doi:10.1002/hipo.20615
46. Coultrap SJ, Nixon KM, Alvestad RM, Fernando Valenzuela C, Browning MD. Differential

- expression of NMDA receptor subunits and splice variants among the CA1, CA3 and dentate gyrus of the adult rat. *Mol Brain Res*. 2005;135(1-2):104-111.  
doi:10.1016/j.molbrainres.2004.12.005
47. Nagy J. Alcohol related changes in regulation of NMDA receptor functions. *Curr Neuropharmacol*. 2008;6(1):39-54. doi:10.2174/157015908783769662
48. Mueller SG, Weiner MW. Selective effect of age, Apo e4, and Alzheimer's disease on hippocampal subfields. *Hippocampus*. 2009;19(6):558-564. doi:10.1002/hipo.20614
49. Pfefferbaum A, Lim KO, Zipursky RB, et al. Brain gray and white matter volume loss accelerates with aging in chronic alcoholics: A quantitative MRI study. *Alcohol Clin Exp Res*. 1992;16(6):1078-1089. doi:10.1111/j.1530-0277.1992.tb00702.x
50. Fama R, Sullivan E V. Thalamic structures and associated cognitive functions: Relations with age and aging. *Neurosci Biobehav Rev*. 2015;54(2):29-37.  
doi:10.1016/j.neubiorev.2015.03.008
51. Hughes EJ, Bond J, Svrckova P, et al. Regional changes in thalamic shape and volume with increasing age. *Neuroimage*. 2012;63(3):1134-1142. doi:10.1016/j.neuroimage.2012.07.043
52. Saygin ZM, Kliemann D, Iglesias JE, et al. High-resolution magnetic resonance imaging reveals nuclei of the human amygdala: manual segmentation to automatic atlas. *Neuroimage*. 2017;155(May 2016):370-382. doi:10.1016/j.neuroimage.2017.04.046
53. Makris N, Gasic GP, Seidman LJ, et al. Decreased absolute amygdala volume in cocaine addicts. *Neuron*. 2004;44:729-740. [https://ac.els-cdn.com/S0896627304006907/1-s2.0-S0896627304006907-main.pdf?\\_tid=b73fc80e-cf42-11e7-8cea-00000aab0f01&acdnat=1511327290\\_ddb61ff9f404958a105c086caf342b95](https://ac.els-cdn.com/S0896627304006907/1-s2.0-S0896627304006907-main.pdf?_tid=b73fc80e-cf42-11e7-8cea-00000aab0f01&acdnat=1511327290_ddb61ff9f404958a105c086caf342b95).
54. Hill SY, De Bellis MD, Keshavan MS, et al. Right amygdala volume in adolescent and young adult offspring from families at high risk for developing alcoholism. *Biol Psychiatry*. 2001;49(11):894-905. doi:10.1016/S0006-3223(01)01088-5
55. Wassum KM, Izquierdo A. The basolateral amygdala in reward learning and addiction. *Neurosci Biobehav Rev*. 2015;57:271-283. doi:10.1002/cnrc.27633.Percutaneous
56. Koob GF. Brain stress systems in the amygdala and addiction. *Brain Res*. 2009;1293:61-75.  
doi:10.1016/j.brainres.2009.03.038
57. Turner JA. The rise of large-scale imaging studies in psychiatry. *Gigascience*. 2014;3(29):1-8.  
doi:10.1186/2047-217X-3-29
58. Lai HMX, Cleary M, Sitharthan T, Hunt GE. Prevalence of comorbid substance use, anxiety

and mood disorders in epidemiological surveys, 1990-2014: A systematic review and meta-analysis. *Drug Alcohol Depend.* 2015;154:1-13. doi:10.1016/j.drugalcdep.2015.05.031

59. Schmaal L, Veltman DJ, van Erp TGM, et al. Subcortical brain alterations in major depressive disorder: findings from the ENIGMA Major Depressive Disorder working group. *Mol Psychiatry.* 2016;21(6):806-812. doi:10.1038/mp.2015.69

**Table 1.** Demographics of non-dependent controls and individuals with a substance dependence, across Models I - III (Mean (SD))

<b>I</b>	<b>Non-dependent controls</b>	<b>Dependent users<sup>a</sup></b>				
	<i>N</i> = 1535	<i>N</i> = 2270				
Sex (M/F %)	58.5/41.5	66.4/33.6*				
Age (Years)	27.5 (9.9)	32.7 (10.7)*				
ICV (10 <sup>6</sup> ) <sup>b</sup>	1.44 (0.23)	1.49 (0.22)*				
<b>II</b>	<b>Non-dependent controls</b>	<b>AlcD</b>	<b>NicD</b>	<b>CocD</b>	<b>MetD</b>	<b>CbD</b>
	<i>N</i> = 1535	<i>N</i> = 830	<i>N</i> = 565	<i>N</i> = 309	<i>N</i> = 171	<i>N</i> = 210
Sex (M/F %)	58.5/41.5	65.4/34.6*	57.5/42.5	78.3/21.7*	66.7/32.6*	69.5/30.5*
Age (Years)	27.5 (9.9)	32.9 (11.3)*	31.1 (9.9)*	39.1 (8.1)*	31.1 (9.1)*	25.6 (9.3)*
ICV (10 <sup>6</sup> )	1.44 (0.23)	1.53 (0.22)*	1.48 (0.22)*	1.41 (0.20)	1.55 (0.16)*	1.51 (0.19)*
<b>III</b>	<b>Non-smoking controls</b>	<b>Smoking controls</b>	<b>NicD</b>			
	<i>N</i> = 918	<i>N</i> = 189	<i>N</i> = 565			
Sex (M/F %)	61.1/38.9	64.0/36.0	57.5/42.5			

Age (Years)	29.7 (9.6)	28.9 (9.4)	31.1 (9.9)*
ICV (10 <sup>6</sup> )	1.41 (0.24)	1.52 (0.20)*	1.48 (0.22)*

<sup>a</sup>Substance dependence include AlcD = alcohol, NicD = nicotine, CocD = cocaine, MetD = meth, and Cbd = cannabis dependence

<sup>b</sup>ICV = intracranial volume, measured in mm<sup>3</sup>

\* $p < .05$ . Each dependent group was compared against non-dependent controls (or non-smoking controls in Model III) with  $t$ -tests for Age and ICV and  $\chi^2$  tests for Sex.

**Table 2.** Significant regions (as percentage of vertices, %) and average effect size ( $d$ ) of differences in radial distance (RD) and Jacobian determinant (JD) common across splits 1 and 2, across Models I – III.

Model	Contrast	Region	Radial Distance (RD)				Jacobian Determinant (JD)				
			Percentage of total region (%)	$d^*$	$d_{raw}^*$	$p$	Percentage of total region (%)	$d^*$	$d_{raw}^*$	$p$	
I	Dependent users vs. non-dependent controls	Left	Amygdala	0	-	=	-	0.66	-0.128	<u>-0.141</u>	0.009
			Hippocampus	3.24	-0.146	<u>-0.162</u>	0.005	28.70	-0.155	<u>-0.169</u>	0.005
			Thalamus	0.04	-0.127	<u>-0.167</u>	0.008	0.36	-0.152	<u>-0.177</u>	0.003
		Right	Accumbens	10.65	-0.143	<u>-0.174</u>	0.005	0	-	=	-
			Amygdala	3.51	-0.172	<u>-0.178</u>	0.002	7.02	-0.149	<u>-0.148</u>	0.004
			Hippocampus	1.04	-0.146	<u>-0.137</u>	0.004	22.06	-0.164	<u>-0.171</u>	0.003
			Putamen	0	-	=	-	0.76	-0.150	<u>-0.181</u>	0.004

			Thalamus	1.76	-0.138	<u>-0.154</u>	0.005	2.32	-0.167	<u>-0.163</u>	0.002
II	Alcohol-	Left	Hippocampus	4.68	-0.168	<u>-0.188</u>	0.004	31.53	-0.170	<u>-0.184</u>	0.004
	dependent		Putamen	6.59	-0.155	<u>-0.153</u>	0.005	3.68	-0.143	<u>-0.173</u>	0.006
	users vs.	Right	Accumbens	0	-	=	-	1.94	-0.156	<u>-0.188</u>	0.004
	non-		Amygdala	9.28	-0.163	<u>-0.165</u>	0.004	7.38	-0.158	<u>-0.163</u>	0.005
	dependent		Hippocampus	4.64	-0.160	<u>-0.168</u>	0.003	29.30	-0.172	<u>-0.177</u>	0.003
	controls		Putamen	14.91	-0.155	<u>-0.201</u>	0.004	9.11	-0.156	<u>-0.199</u>	0.004
			Thalamus	8.63	-0.166	<u>-0.167</u>	0.004	16.39	-0.154	<u>-0.175</u>	0.004
III	Nicotine-	Left	Amygdala	0.95	0.137	<u>0.112</u>	0.006	0	-	=	-
	dependent		Hippocampus	5.84	0.150	<u>0.167</u>	0.005	45.24	0.166	<u>0.173</u>	0.003
	users vs.		Putamen	6.75	0.155	<u>0.181</u>	0.004	6.59	0.158	<u>0.183</u>	0.003
	non-		Thalamus	0	-	=	-	3.60	0.153	<u>0.160</u>	0.003
	smoking	Right	Accumbens	3.55	0.161	<u>0.182</u>	0.003	9.14	0.141	<u>0.166</u>	0.006
	controls		Amygdala	1.10	0.148	<u>0.167</u>	0.003	0	-	=	-
			Caudate	0.28	0.140	<u>0.186</u>	0.004	0	-	=	-
			Hippocampus	0.40	0.150	<u>0.158</u>	0.004	5.68	0.159	<u>0.158</u>	0.003
			Putamen	1.20	0.135	<u>0.160</u>	0.006	2.64	0.140	<u>0.165</u>	0.006

		Thalamus	9.11	0.157	<u>0.160</u>	0.003	7.43	0.165	<u>0.159</u>	0.002
Smoking controls	Left	Hippocampus	3.92	0.194	<u>0.218</u>	0.004	29.06	0.202	<u>0.227</u>	0.005
		Putamen	0.80	0.201	<u>0.247</u>	0.002	2.72	0.188	<u>0.234</u>	0.005
vs. non- smoking controls	Right	Thalamus	0.03	0.189	<u>0.240</u>	0.004	2.32	0.182	<u>0.219</u>	0.006
		Accumbens	13.23	0.195	<u>0.238</u>	0.005	2.69	0.201	<u>0.141</u>	0.003
		Amygdala	0	-	=	-	0.365	0.207	<u>0.193</u>	0.002
		Hippocampus	0.68	0.205	<u>0.193</u>	0.002	9.67	0.210	<u>0.215</u>	0.004
		Pallidum	0	-	=	-	0	-	=	-
		Putamen	0	-	=	-	0.40	0.175	<u>0.231</u>	0.007
		Thalamus	4.52	0.193	<u>0.210</u>	0.004	5.875	0.214	<u>0.222</u>	0.002

\*Average effect size ( $d$ ) computed over remaining significant regions after overlap of splits 1 and 2. Raw effect size ( $d_{raw}$ ) represents effect size without correcting for covariates (age, sex, intracranial volume)

### Figure Legend

**Fig. 1. Overview of the vertex-wise shape metrics employed.** (A) 3D model of subcortical structures within the brain space. (B) The radial distance (RD) of a structure corresponds to the distance between each surface vertex and the structure's medial skeleton. (C) The Jacobian

determinant (JD) corresponds to the deformation necessary to match the subject-specific structure to a template. A higher JD reflects a larger 'surface area' relative to the template.

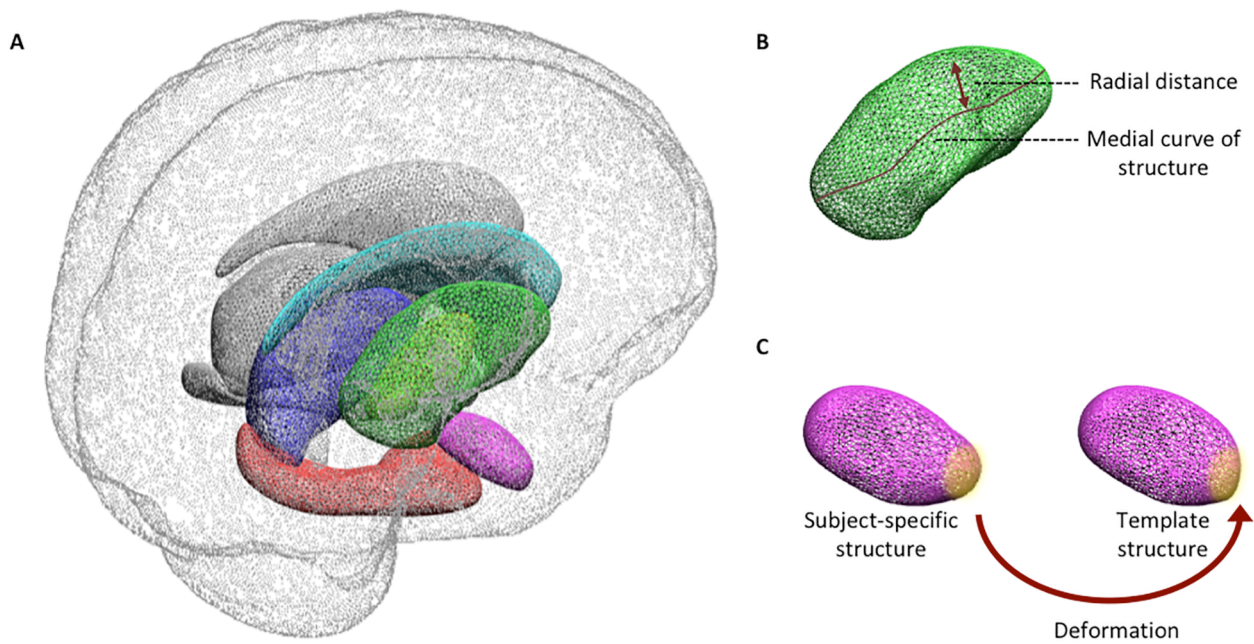
**Fig. 2. Subcortical difference between individuals with substance dependence and non-dependent controls.** Bottom and top view of (i) local surface thickness (radial distance, RD) and (ii) local area (natural logarithm of the Jacobian determinant, JD) differences across subcortical structures in the left (left) and right hemispheres (right), in individuals with substance dependence compared to non-dependent controls. All effects controlled for imaging site, sex, and age. Heat maps represent beta-values of the significant regions in each split half (SPLIT 1 and SPLIT 2). Overlap in significance across both splits are colored in blue in the last column (OVERLAP).

**Fig. 3. Subcortical difference between individuals with alcohol dependence and non-dependent controls.** Bottom and top view of (i) local surface thickness (radial distance, RD) and (ii) local area (natural logarithm of the Jacobian determinant, JD) differences across subcortical structures in the left (left) and right hemispheres (right), in individuals with an alcohol dependence (AlcD) compared to non-dependent controls. All effects controlled for imaging site, sex, and age. Heat maps represent beta-values of the significant regions in each split half (SPLIT 1 and SPLIT 2). Overlap in significance across both splits are colored in blue in the last column (OVERLAP).

**Fig. 4. Subcortical difference between individuals with nicotine dependence and non-smoking controls.** Bottom and top view of (i) local surface thickness (radial distance, RD) and (ii) local area (natural logarithm of the Jacobian determinant, JD) differences across subcortical structures in the left (left) and right hemispheres (right), in individuals with a nicotine dependence (NicD) compared to non-smoking controls.

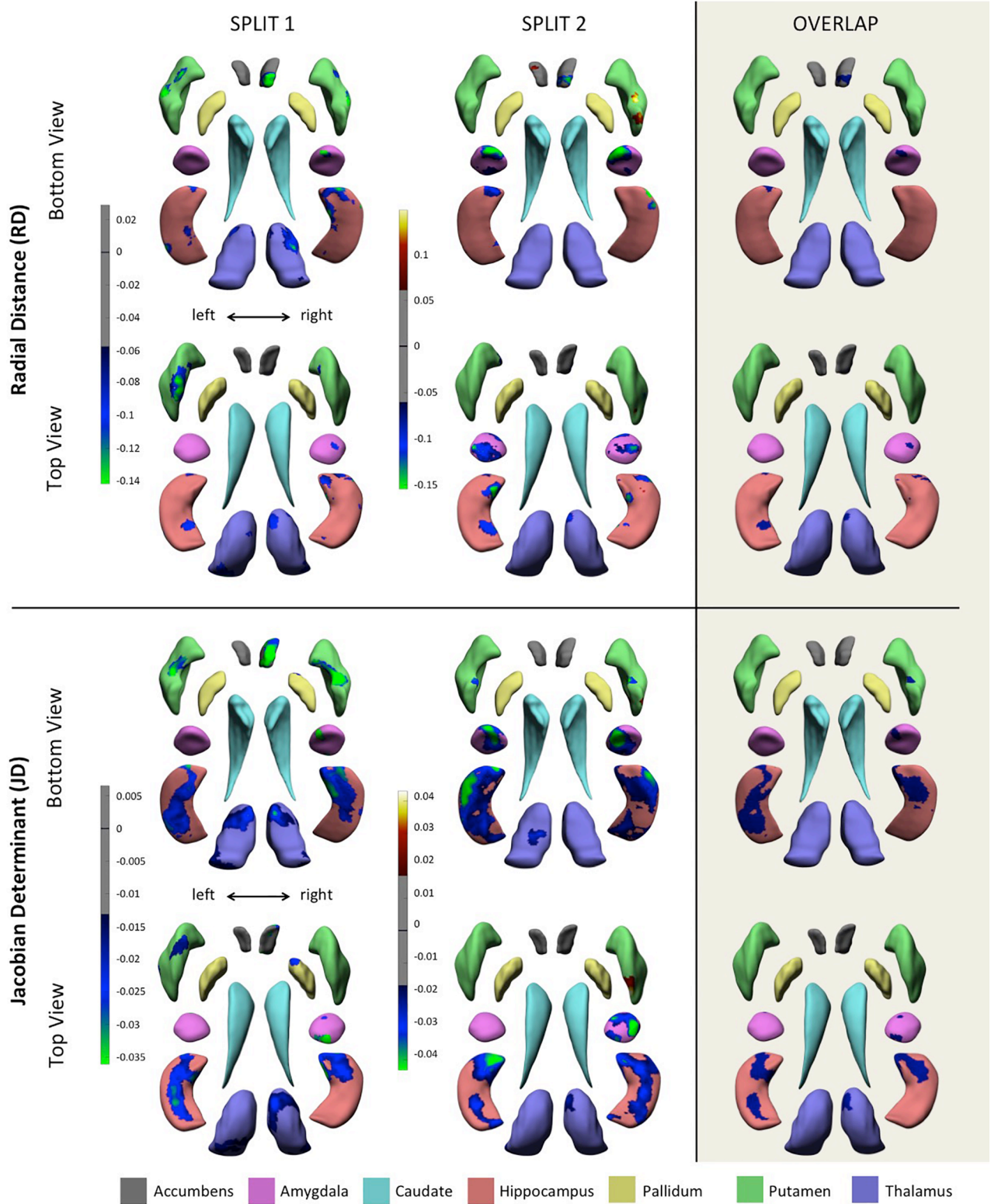
All effects controlled for imaging site, sex, and age. Heat maps represent beta-values of the significant regions in each split half (SPLIT 1 and SPLIT 2). Overlap in significance across both splits are colored in blue in the last column (OVERLAP).

**Fig. 5. Subcortical difference between smoking controls and non-smoking controls.** Bottom and top view of (i) local surface thickness (radial distance, RD) and (ii) local area (natural logarithm of the Jacobian determinant, JD) differences across subcortical structures in the left (left) and right hemispheres (right), in smoking controls compared to non-smoking controls. All effects controlled for imaging site, sex, and age. Heat maps represent beta-values of the significant regions in each split half (SPLIT 1 and SPLIT 2). Overlap in significance across both splits are colored in blue in the last column (OVERLAP).



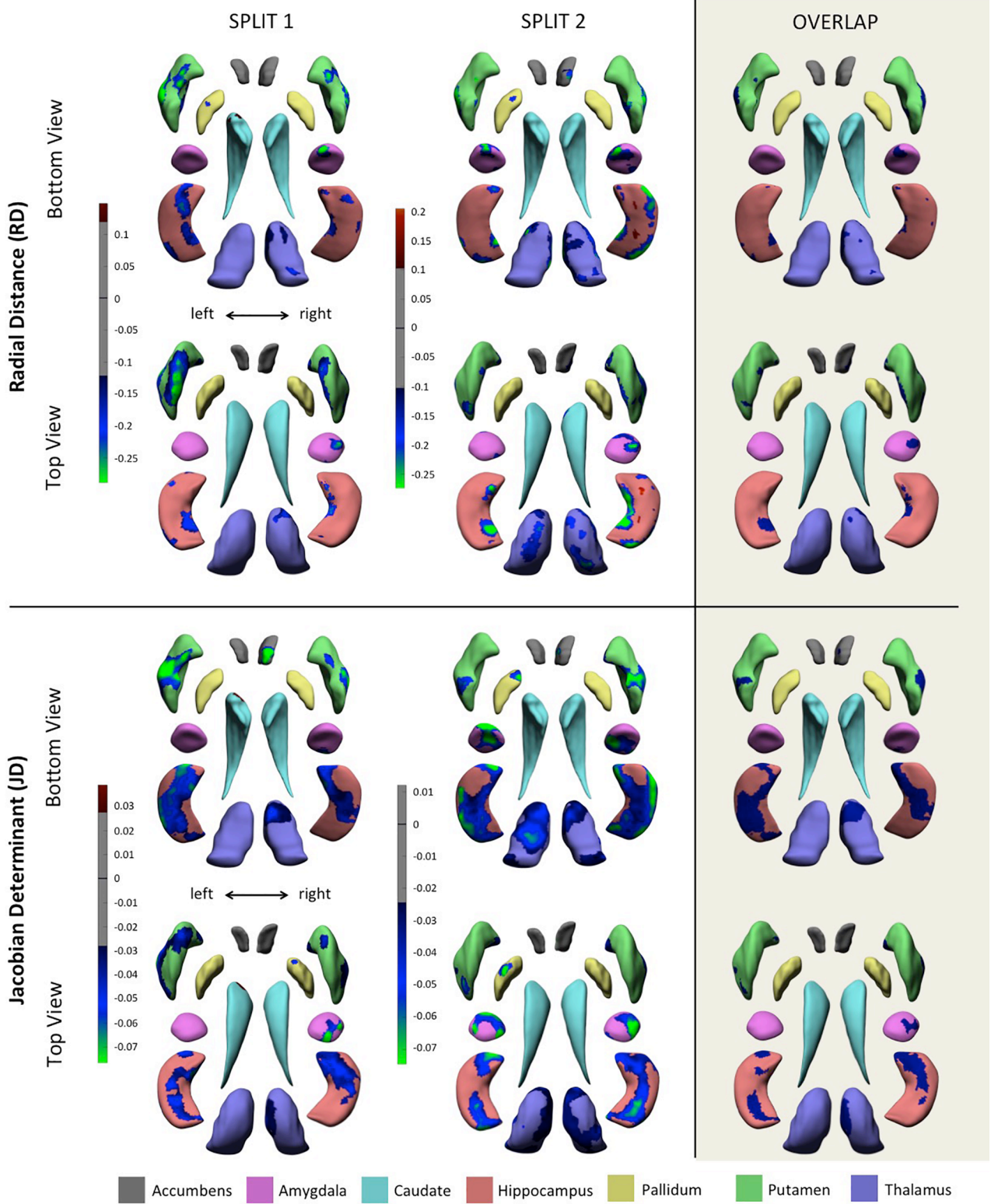
ADB\_12830\_F1.tif

DEPENDENT USERS VS. NON-DEPENDENT CONTROLS



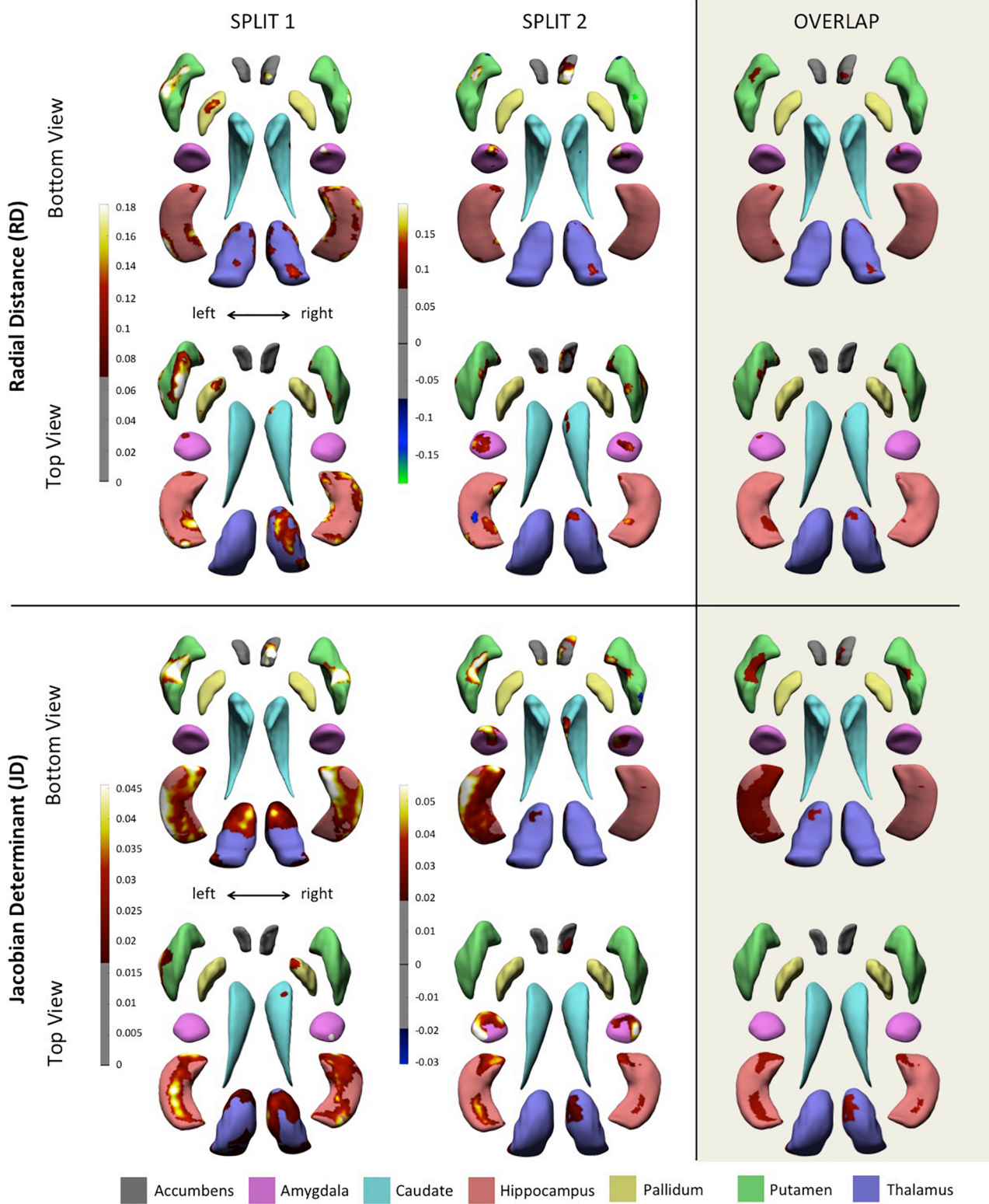
ADB\_12830\_F2.tif

ALCOHOL-DEPENDENT USERS VS. NON-DEPENDENT CONTROLS



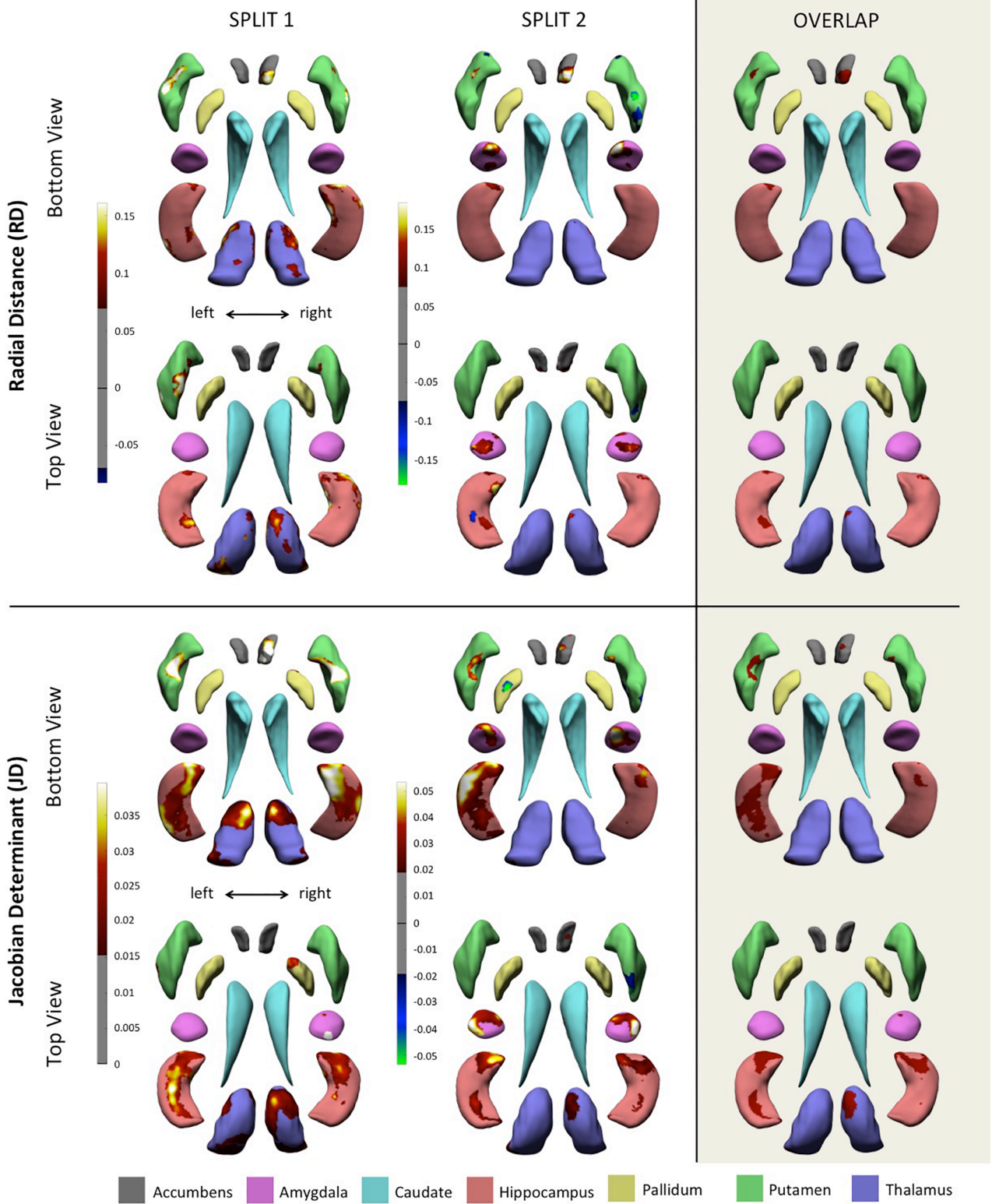
ADB\_12830\_F3.tif

NICOTINE-DEPENDENT USERS VS. NON-SMOKING CONTROLS



ADB\_12830\_F4.tif

**SMOKING CONTROLS VS. NON-SMOKING CONTROLS**



ADB\_12830\_F5.tif